ENVIRONMENTAL TOBACCO SMOKE DEPOSITION OF A PARTICULATE MATTER SAMPLING DEVICE

JENNIFER THOMPSON, RICHARD BARTLETT, AND JUDITH COHEN

This paper would typically be preceded by a title page and an abstract. They are not included here in the interest of space.

INTRODUCTION

Particulate matter (PM) is comprised of both solid and liquid particles that are suspended by gas molecules in the air. The composite mix of PM and the air in which it is suspended is defined as an aerosol. According to the U.S. Environmental Protection Agency (EPA), PM-2.S and PM-10, particles with aerodynamic diameters less than 2.5 and 10 μm, respectively, can cause adverse health effect s with even short-term exposure. Environmental tobacco smoke (ETS) exposure increases the risk for respiratory diseases and lung cancer. The involuntary exposure for children (through secondhand smoke) causes lower respiratory illness in their infancy and early childhood and adverse effects on lung function throughout childhood [1]. Given the important public health implications of PM exposure, a continued need exists for development of cost effective, accurate, and practical measurement devices [2]. Various prototype instruments are being developed to measure the mass, size, and chemical composition of PM to obtain a better assessment tool to remedy misclassification of ETS exposure in epidemiological studies [1]. This device measures particle phase ETS and gas phase (nicotine and 3-ethenyl pyridine) ETS exposure. This portion of the project focused on the ETS deposition mechanism of the particle phase sampling device.

The use of van der Waals induced dipole-dipole attraction is sufficient for surface retention of micron and sub-micron sized particles. Thermophoresis, the normal force on a

particle created by the momentum transfer along the decreasing direction of a thermal gradient (∇T) is an effective method for particle collection in validating traditional methods [3], [4]. When an aerosol is flowing in a narrow channel, the ∇T strength determines the strength of thermophoretic (TP) forces on the particles.

Experiments were conducted with a new device developed to sample airborne particles in indoor air with support from the California Tobacco Related Disease Research Program (TRDRP). Seeking a better understanding of thermophoresis to improve the collection efficiency became a motivation for exploring the theories dealing with TP particle deposition in laminar flow regimes in ducts (~500 μm high). In a series of particle phase experiments using a TP ETS sampler, the TP voltage that controls its ∇T in the sampler was increased until the optimal (maximal) ETS deposition was determined.

The Brock-Talbot model for TP deposition [5] was previously used for proof of concept. In this project, this model was extended over a larger particle size range and compared theoretical predictions with the experimental performance of the TP ETS sampler. The sampler used 25 μm diameter TP wires (California Fine Wire Co., Grover Beach, CA, Nickel Alloy 120) to heat the surrounding air by applying a voltage across the wires. Prior to computer simulation and chamber experiments, the TP wires were arbitrarily set at 1.0 V. Since the wire temperature was proportional to the applied voltage, establishing their relationship was useful for obtaining optimal collection.

MATERIALS AND METHODS

Theoretical Model

In the presence of a ∇T, thermophoresis becomes significant in influencing particle motion [6]. Using the appropriate gradient and particle size range, the collection can be 100% efficient [3]. The TP force is effective for depositing tiny particles flowing through a channel onto a cooler surface. Other parameters such as thermal conductivity, dimension of the flow channel, and viscosity of the particle stream play important roles.

The Brock-Talbot TP force model given by He and Ahmadi [5] is

$$F_{th} = 2C_s C_c \tfrac{1}{\tau} \nu H \frac{\nabla T}{T} m \tag{1}$$

where C_s. is the thermal slip coefficient, and C_c is the Stokes-Cunningham slip correction

$$C_c = 1 + \frac{2\lambda}{d}\left(1.257 + 0.4^{-1.1\frac{d}{2\lambda}}\right) \tag{2}$$

and τ is the relaxation time in Equation (1) given by

$$\tau = \frac{Sd^2 C_c}{18\nu} \tag{3}$$

S is the ratio of particle density to fluid density [7]. T and ∇T are the room temperature and thermal gradient; m is the unit mass and ν is the kinematic viscosity of the molecules. H is the molecular accommodation coefficient given by

$$H = \left(\frac{1}{1+3C_m Kn}\right)\left(\frac{\frac{k_a}{k_p} + C_t Kn}{1 + 2\frac{k_a}{k_p} + 2C_t Kn}\right) \tag{4}$$

This equation indicates the relationship between particle diameter and thermal conductivity. Talbot found these values: C_s= 1.17, C_t=2.18, and C_m=1.14. C_t relates to temperature jump [5],

C_m is the momentum exchange coefficient that depends on the particle-gas configuration [5], [7], and Kn=2 λ/d is the Knudsen number (λ is the mean free path of air and d is particle diameter; k_a and k_p are the thermal conductivity of gas (air) and particles).

The TP collection ratio

$$\eta = \frac{UL}{2hu_m} \tag{5}$$

is the ratio of the TP velocity and the mean air velocity u_m of the channel. L and h, the length and the height of the channel, were set at 71.0 mm and 0.5 mm for the simulation, reflecting the dimensions of the TP ETS sampler. U is the TP velocity

$$U = \frac{F_{th}}{m}\tau \tag{6}$$

which in effect determines the TP collection ratio. Substitute τ and H into Equation (1) and expand in terms of its dependent parameters, and the equation becomes

$$F_{th} = 36C_s \frac{\nu^2}{Sd^2}\left(\frac{1}{1+3C_m Kn}\right)\left(\frac{\frac{k_a}{k_p}+C_t Kn}{1+2\frac{k_a}{k_p}+2C_t Kn}\right)\frac{\nabla T}{T}m \tag{7}$$

The Cs are collectively referred to as the drag forces. One can see that the TP force strength is inversely dependent on particle diameter and the temperature of forming the ∇ T, where ν and k_a/k_p account for the type of particles. This equation is simulated with the molecular diameter of air at 5.7 nm, and the aerosol particles consist of NaCl with thermal conductivity k_p=6.69 W m^{-1} K^{-1} [5].

Apparatus

The collection apparatus consists of a loom-like frame machined from a copper clad printed circuit board that holds a set of TP wires and acts as a flow channel, and a mounting

surface for fin-cooled aluminum particle collection surfaces. The device becomes an airtight flow-through channel with three sets of TP collection areas. A small pump of flow rate 0.01 L/min pulled a PM-laden air sample through the device. Four fine TP wires of 25 μm in diameter and about 5 mm in length were soldered, physically in parallel and electrically in series, to form a coplanar resistive heater about 5 mm on each side. Three of these heaters created three separate TP collection regions (Figure 1). When a voltage was applied across one of the three wire circuits, a ∇T formed between the wires and the fin-cooled aluminum collection surface.

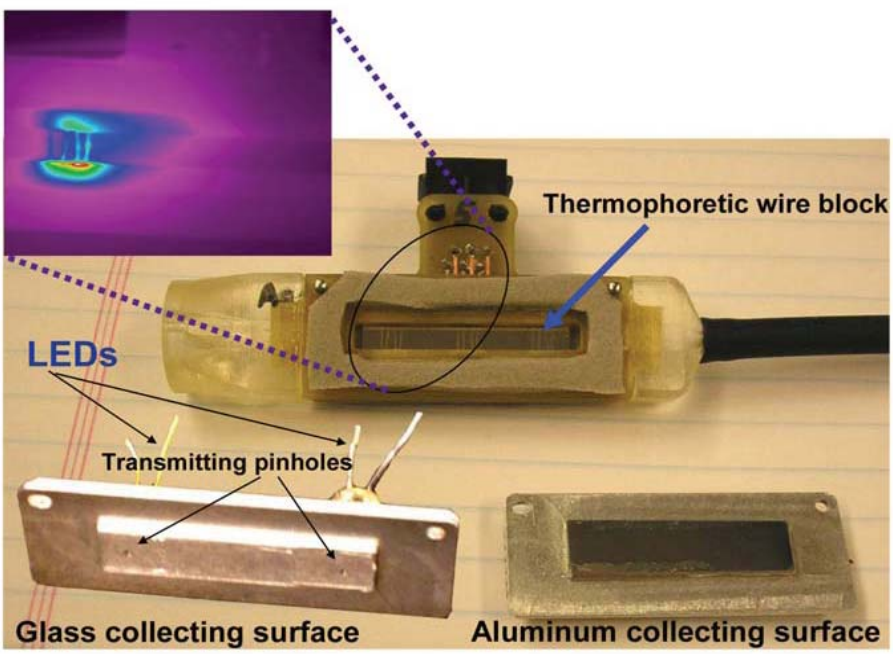

Figure 1: The TP ETS Sampler with thermophoretic wires indicated; glass collecting surface and aluminum collecting surface are separately shown at the left and the right. The thermogram insert shows the heated TP wires region when powered.

Two collecting surface con figurations were used on the two sides of the TP wire blocks for particle collection. An aluminum collection surface (Figure 1) was fabricated with a polished thin aluminum surface attached to an aluminum body with double-sided heat conducting tape. A glass collection surface was assembled with a thin glass cover slide and another aluminum body. The glass cover slide was glued at the edges to allow light transmission through two circular

pinholes of diameter ~1 mm that were each centered on a TP particle deposition area on the surface. LEDs (Roithner Lasertechnik, Vienna, Austria, UV-LED 380D30 and ELD-8l 0-525) of peak wavelength 380 nm (UV) and 810 nm (IR) were inserted into the back of the surface so a light beam traveled through the pinholes and emerged normal to the glass. The pinholes were centered on the TP deposition surfaces for two of the three areas on the glass-covered collection body.

Thermophoretic Wire Temperature

In Figure 1. the thermogram insert shows the heated TP wires. Due to the low emissivity of the wires, the thermogram merely indicates the wires were hotter than their surroundings when powered, yet does not accurately indicate the *exact* temperature. Using an alternate approach to thermography, the approximate temperature of the TP wire could be calculated in terms of resistance with the known temperature coefficient of resistance of the TP wire provided by the manufacturer. A 50 x 50 x 80 cm convection oven measured the temperature resistance of the TP wires. A differential temperature controller gradually raised the temperature while two small 12 V fans mixed air inside the oven. A sampler was placed inside the oven to measure resistance of two blocks of TP wires. Using Ohm's law, measuring the resultant voltage vs. temperature relationship was possible, for the temperature associated with experimental voltage and current.

Experiment Setup and ETS Genera/ion

A 24 m^3 environmental chamber was built with a wood frame, wallboard walls and ceiling, and magnetic refrigerator door seals. Low volatile organic compound emitting paints and sealants was applied inside the chamber to minimize unwanted room-ambient particles and volatile organic compounds [8]. The chamber was bolted stationary in a one-story building, no

ventilation equipment was used, and the room temperature stayed approximately steady during the sampling periods. The TP ETS sampler was hung from a stand 0.5 m above the floor, side by side with the a Personal Environmental Monitor (PEM) PM-2.5 sampler (SKC Inc., Eighty Four, PA, 761-203). The PEM, assembled with a Teflon-coated fiberglass filter (SKC Inc., Eighty Four, PA, SKC Filter 761 -203) and sampling at a rate of2.0 L/min, provided the integrated PM mass concentration in the chamber during the sampling period. Using the proportionality of the integrated PM mass concentration and TP ETS sampler flow rates, the total particle mass that traversed the TP ETS sampler during operation was calculated.

ETS was generated by concurrently and completely smoldering eight cigarettes for each run. ETS is a complex mixture of solid and vapor phase particles produced primary from the burning of cigarettes and depends on pufTrate [8]. The TP ETS sampler validation was focused on the deposition mechanism, thus smoldering cigarette smoke was effective and appropriate for these experiments. The TP ETS sampler controller microprocessor was programmed to switch amongst the three sampler TP wire regions in a reverse sequence fashion (i.e., 1-2-3,3-2-1, 1-2-3, ..) every 5 minutes. The purpose of this was to avoid collection bias during decay of the aerosol concentration in the chamber, and therefore this non-random sampling pattern distributed near-equal particle mass collection on each of the three regions of the sampler's collection surfaces. A series of experiments was conducted at increasing wire voltage settings from the pre-set voltage of 1.0 V to the optimal voltage where a maximum particle collection value (Table 1) was reached. The voltage and current inputs of each wire were recorded for analysis. Each experiment was allowed to collect for at least 17 hours in order to obtain significant amounts of ETS.

TP Voltage and Related Thermal Parameters			
TP Voltage [V]	Resistance [Ω]	T [ºC]	∇T [K/cm]
1.0	13.6	107	1740
1.5	15.4	179	5190
2.0	18.3	252	4640
2.5	19.5	325	6090
3.0	25.2	397	7540

Table 1: The corresponding thermal parameters of the TP voltages used for experiments.

Thermal Conductivity Ratio (k_p/k_a) of Several Materials	
Materials	Unitless ***kp/ka***
Air at 20 ºC	1
Asbestos	3
Paraffin oil	5
Magnesium oxide	5
Stearic acid	5
Castor oil	7
Water	23
Clay	27
Glass	32
Fused silica	38
Granite	81
Carbon	169
Sodium chloride	254
Mercury	323
Quartz	369
Iron	2573

Table 2: Ratio of thermal conductivity of several materials to of air can be found in ambient air. k_p and k_a values were adopted from Ref. 3.

Spectrometry and Related Statistics

The samples on the glass slide collection surface were then examined by using fiber optic probes connected to a UV-NIR spectrometer (Ocean Optics, Dunedin. FL. S2000 UV-VIS 250-8oonm). Figure 2 shows the schematic of the operation when the UV LED was powered. The

LEDs were placed on a light-tight housing and connected to an external power supply. With the LEDs turned on, UV or NIR light was transmitted through the cover slide. Fiber optic probes were attached to the bottom of the housing cavity and connected via a channel selector to the spectrometer. After ETS was collected on the glass cover slide the sample spectrum was recorded. Next, the ETS sample was removed by cleaning off the glass collection surface to obtain the baseline spectrum. The absorbance was calculated with Beer's Law, $A = -\log(I/ I_o)$, where I and I_o were the calculated peak intensities of the spectrum taken by a spectrometer.

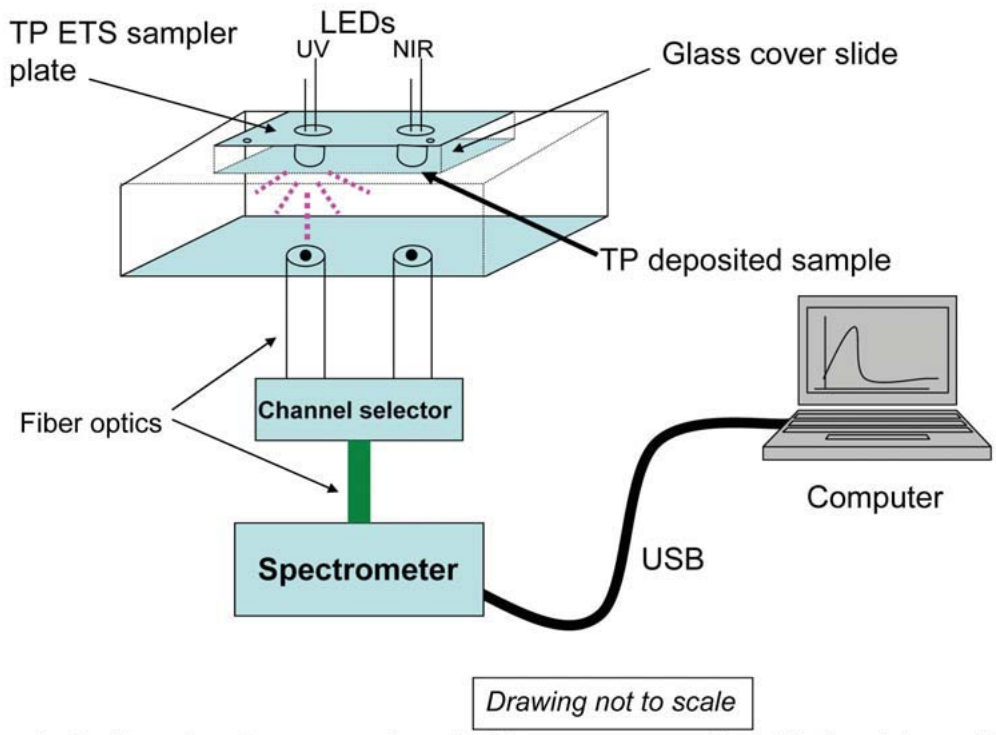

Figure 2: Configuration of spectrometric method for measurement of particle deposition on TP ETS Sampler.

To account for small differences between ETS concentrations in each experiment, the calculated ETS absorbance was normalized by the integrated ETS concentration from the PEM during the sampling period in order to determine collection efficiency in terms of mass. The UV absorbance results were much more robust than those from the NIR LED since ETS has strongly

enhanced UV absorbance. The NIR absorbance measurements in the case of these ETS samples were typically below the limit of quantitation for the method, making them of little use in this investigation. The filter mass collected by PEM Tenon-coated fiberglass filter was first measured with an electronic microbalance, and then the air PM concentration was calculated based on the sampling now rate and duration. The ETS mass that entered the TP ETS sampler during each experiment was computed by multiplying the PEM-based PM concentration by the experiment sampling time and sampler flow rate. The TP ETS sampler UV absorbance was normalized to that of a 10 μg mass sampling based on the above calculation.

RESULTS

Collection Ratio

The Brock-Talbot deposition ratio was plotted as a function of aerosol diameter for NaCl in Figure 3a. Figure 3b depicts the influence of the thermal conductivity of different materials on thermophoretic deposition. Table 2 lists the thermal conductivity ratio (k_p/k_a) of several possible material types found in PM. These results taken together show how different types of PM could have different thermal properties that affect the TP collection ratio. Figure 3a shows that the thermophoretic particle deposition ratio is about 0.6 and gradually decreases to 0.1 for the pre-set thermal gradient ($\nabla T = 1600$ K/cm).

(a)

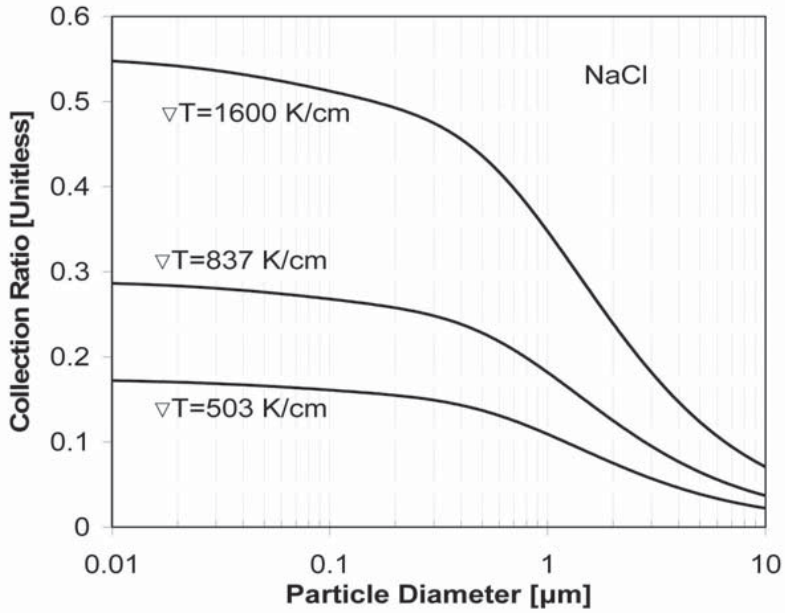

(b)

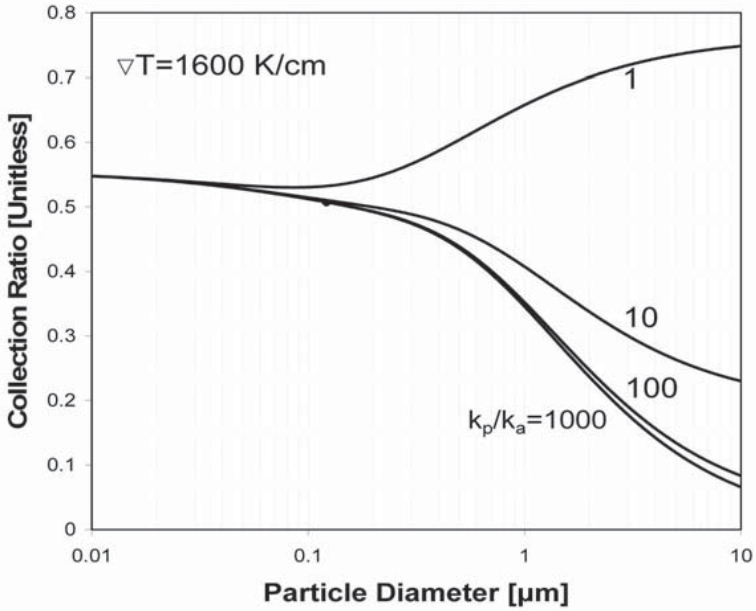

Figure 3: (a). Thermophoretic collection ratio vs. particle diameter using Brock-Talbot model with 3 different thermal gradients. (b). Particle collection ratio vs. diameter for different k_p/k_a using the Brock-Talbot model.

Temperature Correlation

Heating the TP wires generated resistance vs. temperature data aligned with the wire manufacturer's temperature coefficient of resistance (Figure 4a). Each time the voltage applied to the TP wire was recorded, and the correlation to resistance was plotted (Figure 4b). Thus one can obtain the temperature as a function of applied voltage. Combining Figures 4b and 4a, a relationship of $T = 145.1\ V \cdot - 28.5$ (where T is the TP wire temperature (°C) forming the ∇T and V is the applied voltage). Table 1 summarizes the experimental applied voltages and their thermal parameters.

(a)

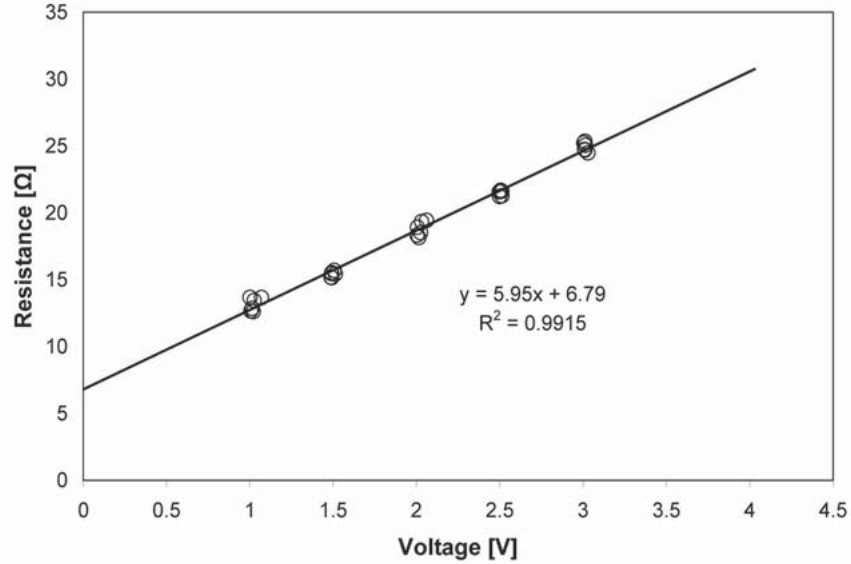

(b)

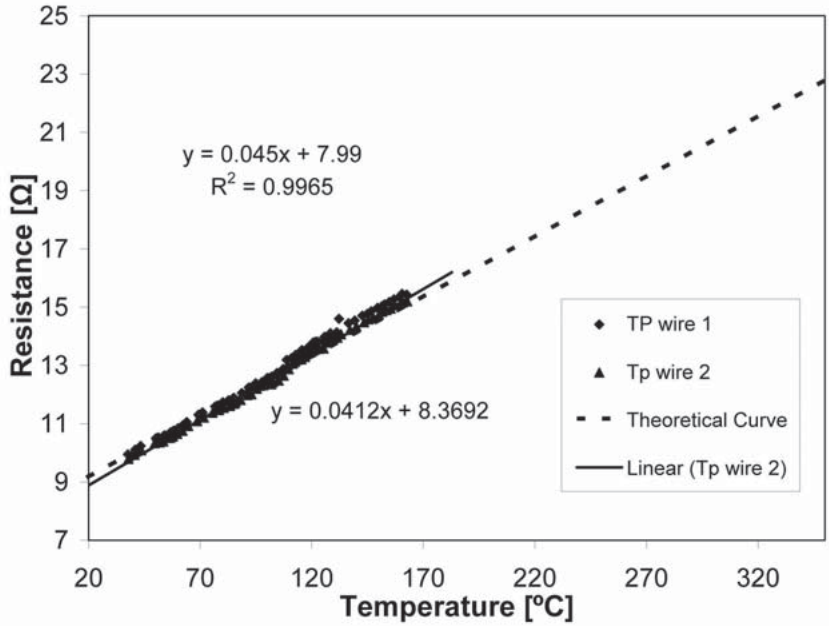

Figure 4: (a). Ten sets of applied TP voltages vs. resistance recorded from chamber experiments, with some of them coincide almost exactly. (b). Two different blocks of wire were heated and their resistances were measured. The dashed line is the curve calculated with manufacture resistance coefficient, α=0.0045, plotted for a wider range than the experimental range.

Normalized Absorbance and Optimal Collection

The chamber experiment data show increased particle collection in terms of absorbance with increasing wire voltage. ETS absorbance measurements from the TP ETS sampler normalized to a 10 μg sample was plotted against TP wire voltage and fined with a 2nd order polynomial (Figure 5). Each data point was obtained by averaging two experiments. Error bars in Figure 5 represent the greatest deviation from the experimental average. The optimal voltage for this ETS sampler was identified between 2.5 and 3.0 V, based on this fit.

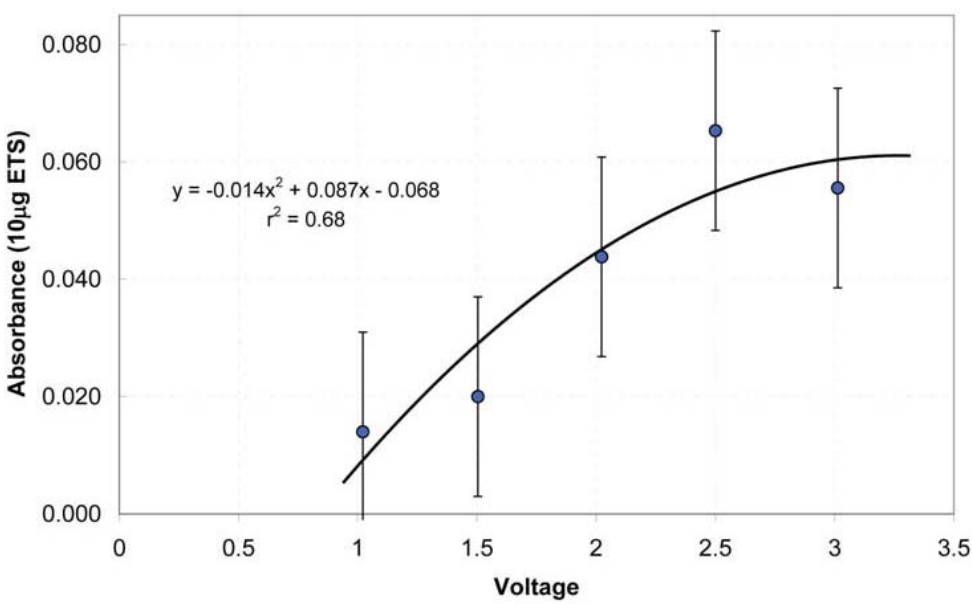

Figure 5: Particle phase titration result shows the optimal collection of the TP ETS sampler is with the input voltage of about 2.5 V; the scattered absorbance data are averaged with two filter mass (PEM) normalized data. Enchantment also suggested a factor of 5 better in collections. The error bars represent the greatest deviation from the experimental average based on two experiments for each voltage.

DISCUSSION AND CONCLUSION

Thermophoretic modeling (Figure 3a) shows effective collection ratio for sub-micron particles. Here, the collection ratio is defined as the ratio of TP velocity to the mean air velocity in the channel, and the collect ion efficiency is the ratio of aerosol being collected to the amount

that flows in the channel. As a remark, one team of scientists [5] called the quantity η, the collection efficiency and multiplied by 100%, and another team [9] called it the collection efficiency and used it as a decimal number. In this chart (Figure 3), the particle collection ratio quickly decreased in the micron region as the diameter increased: (Kn<2) decreased drastically to 0.1 μm. The Brock-Talbot simulation explains that particle deposition will increase substantially as the ∇T rises above ∇T= 1600 K/cm. If the ratio k_p/k_a is small, the diameter of the particle increases Figure 3; conversely, as k_p/k_a increases, the collection ratio decreases drastically (Figure 3b). This result is consistent with the presentation by Hinds describing thermophoretic velocity as a function of k_p/k_a [3].

Based on the Brock-Talbot theoretical prediction, we should expect higher particle deposition for sub-micron sized particles. The calculated ∇T for 2.5 V is about ∇T=6090 K/cm, and the Brock-Talbot model collection ratio for this ∇T is well above 1.0. The original selection for TP voltage of this low·cost particle sampler took into account the power consumption; 1.0 V TP voltage was believed to be above 80% efficient for PM-2.5 collection according to He and Ahmadi's results [5, Figure 9). This study has shown, both numerically and experimentally, the optimal deposition ratio occurs between 2.5 and 3.0 V for this TP ETS sampler. The absorbance at 2.5 V TP collection shows a signal five times stronger than that of 1.0 V (Figure 5). It is obvious that the optimal collection efficiency in term of normalized ETS mass at least factor of 5 higher than ∇T=1 V. Figure 6 shows another relationship of deposition ratio, this verified that the Brock-Talbot model also predicted an enchantment of a factor of 5 (from about 0.5 to 2.5 for a 100 nm particle diameter). This result may provide a useful calibration mechanism for developing the TP ETS sampler.

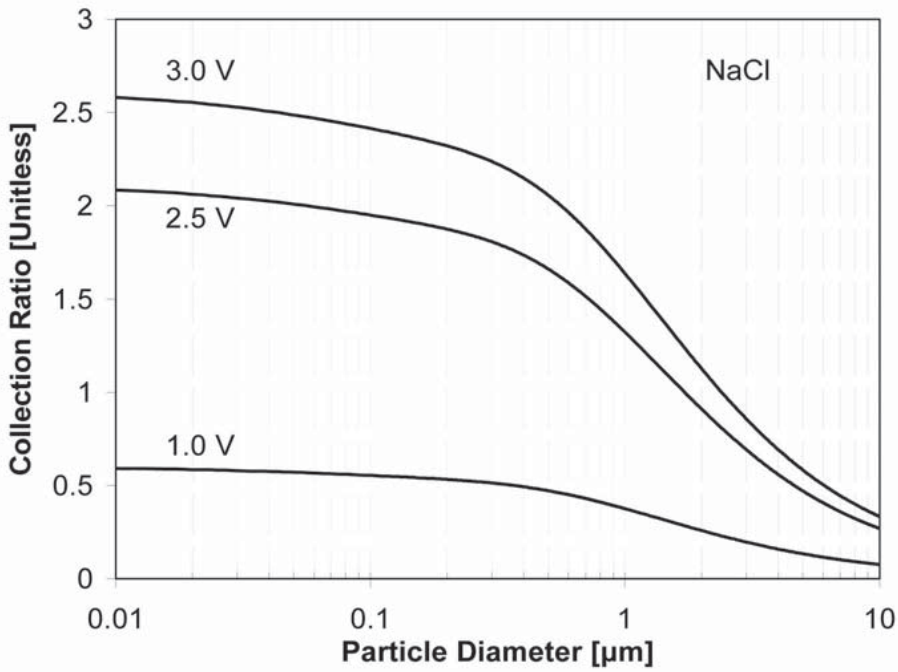

Figure 6: The Brock-Talbot model with thermal gradient corresponding to 1.0 (∇T = 1740 K/cm), 2.5 (∇T = 6090 K/cm), and 3.0 V (∇T = 7540 K/cm) applied voltage (TP gradient). Result shows that 3.0 V applied voltage can collect a factor of 5 more than that of 1.0 V applied voltage.

This project investigated several major issues dealing with the TP ETS sampler particle collection efficiency and identified some important thermal parameters that influence aerosol collection by thermophoresis. This result raised a concern that the oven-treated TP wire temperature may not correctly describe the ∇T of the TP ETS Sampler's *in situ* performance. Calibrating the sampler's ∇T will be helpful because the configuration of TP wires relative to a cool flat collection surface differs from the two-parallel plate configuration used in the Brock-Talbot model [7], [9]. We have shown that the applied voltage for the TP wires should be higher. Moreover, how the TP wire temperature affects the ∇T is unsolved for the configuration of this sampler. This question can be answered with future investigation.

ACKNOWLEDGEMENTS

This work was supported by the Center for Science and Engineering Education at Lawrence Berkeley National Laboratory, U.S. Department of Energy, Office of Science, the California Tobacco Related Disease Research Program and the California Air Resources Board Innovative Clean Air Technologies Program. I would like to thank my mentors Michael Apte and Lara Gundel. I would also like to thank Matt McHugh, David Liedemmn, Rachelle Majeske, and Howdy Goudey for their assistance.

REFERENCES

[1] "The Health Consequences of lnvoluntary Exposure to Tobacco Smoke: A Report of the Surgeon General," U.S. Department of Health and Human Services, Centers for Disease Control and Prevention, Coordinating Center for Health Promotion, National Center for Chronic Disease Prevention and Health Promotion, Office on Smoking and Health, Atlanta, GA: Tech. Rep., 2006.

[2] A. Chung, D.P.Y Chang, M.J. Kleeman, K.D. Perry, T.A. Cahill, D. Dutcher, E.M. MacDougall, and K. Stroud "Comparison of real-time instruments used to monitor airborne particulate matter," *Journal of Air and Waste Management Association*, vol. 51, pp. 109-120, 2001.

[3] W. Hinds, *Aerosol Technology: Properties. Behavior, and Measurement of Airborne Particles,* New York: John Wiley & Sons, 1982.

[4] C.J. Tsai and J. Lin, "Thermophoretic deposition of particles in laminar and turbulent tube flows," *Aerosol Science and Technology*, vol. 38, pp. 131-139, 2004.

[5] C. He and G. Ahmadi, "Particle deposition with thermophoresis in laminar and turbulent duct flows," *Aerosol Science and Technology*, vol. 29, pp. 525-546, 1998.

[6] L. Talbot, R.K. Cheng, R.W Schefer, and D.R. Willis, "Thermophoresis of particles in a heated boundary layer," *Journal of Fluid Mechanics*, vol. 101 **,** pp. 737-758, 1980.

[7] J.R. Brock, "On the theory of thermal forces acting on aerosol particles," *Journal of Colloid Science*, vol. 17, pp. 768-780, 1962.

[8] M.G. Apte and L.A. Gundel, "Indoor measurements of environmental tobacco smoke," Lawrence Berkeley National Laboratory, University of California–Berkeley, CA 94720, Final Report to the Tobacco Related Disease Research Program, LBNL-4914S, 2004.

[9] C.J. Tsai and H.C. Lu, "Design and evaluation of a plate-to-plate thermophoretic precipitator," *Aerosol Science and Technology*, vol. 22, pp. 172-180, 1995.